

# Large-scale model of mammalian thalamocortical systems

Eugene M. Izhikevich and Gerald M. Edelman\*

The Neurosciences Institute, 10640 John Jay Hopkins Drive, San Diego, CA 92121

Contributed by Gerald M. Edelman, December 27, 2007 (sent for review December 21, 2007)

The understanding of the structural and dynamic complexity of mammalian brains is greatly facilitated by computer simulations. We present here a detailed large-scale thalamocortical model based on experimental measures in several mammalian species. The model spans three anatomical scales. (i) It is based on global (white-matter) thalamocortical anatomy obtained by means of diffusion tensor imaging (DTI) of a human brain. (ii) It includes multiple thalamic nuclei and six-layered cortical microcircuitry based on *in vitro* labeling and three-dimensional reconstruction of single neurons of cat visual cortex. (iii) It has 22 basic types of neurons with appropriate laminar distribution of their branching dendritic trees. The model simulates one million multicompartmental spiking neurons calibrated to reproduce known types of responses recorded *in vitro* in rats. It has almost half a billion synapses with appropriate receptor kinetics, short-term plasticity, and long-term dendritic spike-timing-dependent synaptic plasticity (dendritic STDP). The model exhibits behavioral regimes of normal brain activity that were not explicitly built-in but emerged spontaneously as the result of interactions among anatomical and dynamic processes. We describe spontaneous activity, sensitivity to changes in individual neurons, emergence of waves and rhythms, and functional connectivity on different scales.

brain models | cerebral cortex | diffusion tensor imaging | oscillations | spike-timing-dependent synaptic plasticity

The last decade has seen great progress in our understanding of brain dynamics and underlying neuronal mechanisms. Linking these mechanisms to behavior such as perception is facilitated by large-scale computer simulations of anatomically detailed models of the cerebral cortex (1–3). Although these models have stressed microcircuitry and local dynamics, they have not incorporated multiple cortical regions, corticocortical connections, and synaptic plasticity. In the present article, we describe a large-scale model of the mammalian thalamocortical system that includes these components.

Spatiotemporal dynamics of the simulation show that some features of normal brain activity, although not explicitly built into the model, emerged spontaneously. The model exhibited self-sustained activity in the absence of any external sources of input. The behavior of the model was extremely sensitive to contributions of individual spikes: adding or removing one spike of one neuron completely changed the state of the entire cortex in  $<0.5$  s. Regions of the model brain exhibited collective waves and oscillations of local field potentials in the delta, alpha, and beta ranges, similar to those recorded in humans (4). Simulated fMRI signals exhibited slow fronto-parietal anti-phase oscillations, as seen in humans (5).

The shape and connectivity of the model were determined by diffusion tensor imaging (DTI) data for a human brain. Experimental data from three species, human, cat, and rat, were incorporated to build other details of the model.

**Model Structure.** Here, we review some of the basic assumptions used to construct the model, summarized in Figs. 1–3. A full description is provided in [supporting information \(SI\) Appendix](#).

For computational reasons, the density of neurons and synapses per  $\text{mm}^2$  of cortical surface was necessarily reduced. Accordingly,

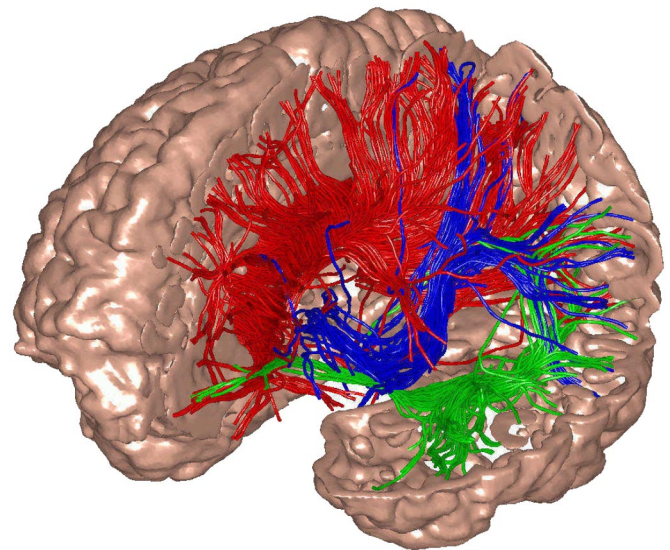


**Fig. 1.** The model's global thalamocortical geometry and white matter anatomy was obtained by means of diffusion tensor imaging (DTI) of a normal human brain. In the illustration, left frontal, parietal, and a part of temporal cortex have been cut to show a small fraction of white-matter fibers, color-coded according to their destination.

the model neurons have fewer synapses and less detailed dendritic trees than those of real cortical neurons. Although we do not explicitly model subcortical structures other than the thalamus, we do simulate brainstem neuromodulation, including the dopaminergic reward system (6, 7) and the cholinergic activating system. Developmental changes, other than activity-dependent fine-tuning of connectivity due to dendritic STDP, are also not modeled explicitly.

**Macroscopic Anatomy.** Diffusion tensor imaging (DTI) data derived from magnetic resonance imaging (MRI) of a human brain was used to identify the coordinates of the cortical surface to allocate cell bodies of model neurons at appropriate locations. Consequently, the model reflects all areas of the human cortex, the folded cortical structure with sulci and gyri. The DTI data, analyzed using the "TensorLine" algorithm (8, 9), formed the white matter tracts of the model, portions of which are illustrated in Fig. 1, that connect individual neurons in one area with target neurons in other areas.

So that neuronal density approached that of animal cortices, spatial scales were reduced by a factor of 4 (so the model cortex

Author contributions: E.M.I. and G.M.E. designed research; E.M.I. performed research; E.M.I. and G.M.E. analyzed data; and E.M.I. and G.M.E. wrote the paper.

The authors declare no conflict of interest.

\*To whom correspondence should be addressed. E-mail: edelman@nsi.edu.

This article contains supporting information online at [www.pnas.org/cgi/content/full/0712231105/DC1](http://www.pnas.org/cgi/content/full/0712231105/DC1).

© 2008 by The National Academy of Sciences of the USA

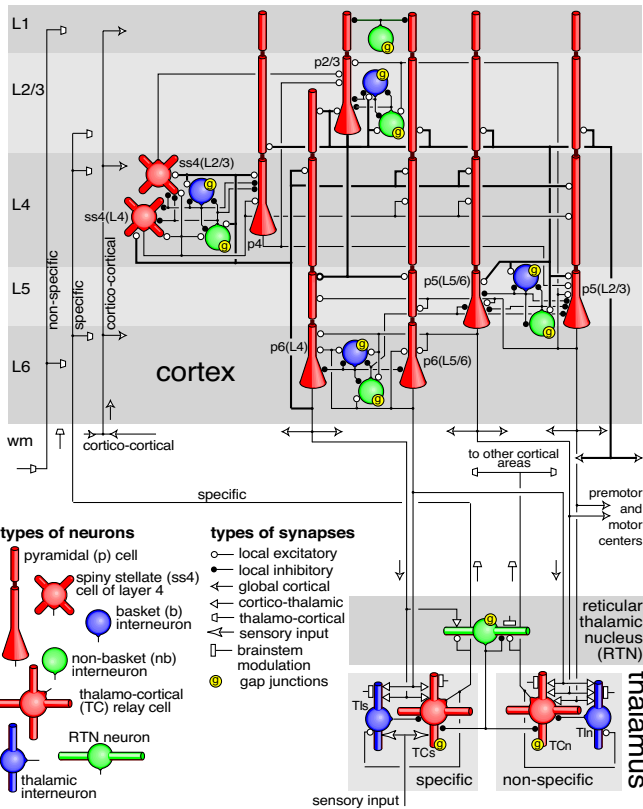


**Fig. 2.** Simplified diagram of the microcircuitry of the cortical laminar structure (*Upper*) and thalamic nuclei (*Lower*). Neuronal and synaptic types are as indicated. Only major pathways are shown in the figure. Complete details are provided in *SI Appendix*. L1-L6 are cortical layers; wm refers to white-matter. Arrows indicate types and directions of internal signals.

diameter was 40  $\mu\text{m}$ ), while relative distances were preserved. The length of the fibers determined axonal conduction delays, which were as long as 20 ms in the model. Because DTI does not presently have sufficient resolution, small bundles of fibers in the human brain were inevitably missed.

**Microscopic Anatomy.** A summary of simulated gray matter microcircuitry is presented in Fig. 2. It is based on the detailed reconstruction studies of cat area 17 (visual cortex) by Binzegger *et al.* (10), whose nomenclature is adapted here. Depending on the morphology (pyramidal, spiny stellate, basket, non-basket), and the somatic and the target layer, we distinguish eight types of excitatory neurons [p2/3, ss4(L4), ss4(L2/3), p4, p5(L2/3), p5(L5/6), p6(L4), p6(L5/6)] and nine types of inhibitory neurons (nb1, nb2/3, b2/3, nb4, b4, nb5, b5, nb6, b6). See *SI Appendix* for a more detailed explanation, in which we provide the matrix of intercortical connectivity and a summary of the magnitudes of laminar axonal spread. Every area of the model cortex had essentially the same microcircuitry as shown in Fig. 2.

The model incorporates specific and nonspecific nuclei of the thalamus, distinguishing two types of excitatory thalamocortical neurons (TCs, TCn) and two types of thalamic inhibitory interneurons (TIs, TIIn) as well as the inhibitory neurons of the reticular thalamic nucleus (RTN). Axonal arborizations and projection patterns of thalamic neurons were all similar to those reported for LGN (see *SI Appendix*).

**Branching Dendritic Trees.** Each neuron in the model has a somatic compartment and a number of dendritic compartments, with at least one apical compartment per cortical layer (if the dendritic tree

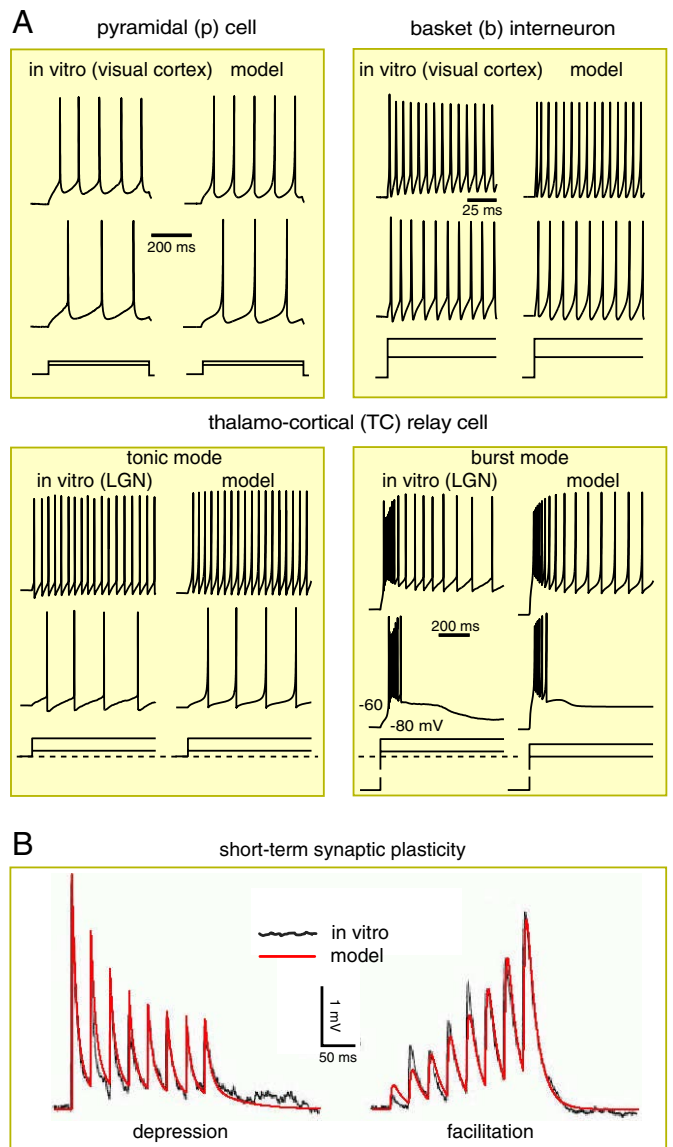


**Fig. 3.** Firing patterns and short-term synaptic plasticity. (A) Comparisons of four representative firing patterns recorded *in vitro* (*Left* columns) and simulated (*Right* columns) using the phenomenological model (1, 2). Different neuronal types have different values of parameters; see *SI Appendix*. (B) Comparison of short-term synaptic plasticity recorded *in vitro* (black noisy curve; modified from figure 4 of ref. 16) and simulated (red smooth curve) by the model (3).

extends to that cortical layer). The exact number of dendritic compartments for each neuron was determined dynamically (see *SI Appendix*) during the initialization procedure, maintaining 40 or fewer synapses per compartment.

In most cases, firing of an excitatory presynaptic neuron evoked a local EPSP in the postsynaptic dendritic compartment of  $<10$  mV amplitude. Such dendritic EPSPs typically result in a submillivolt EPSP at the somatic compartment because of electrotonic attenuation of synaptic current. Coincident firing of three or four synapses with maximal conductances in the same compartment can result in a local dendritic action potential (spike), which then can propagate to the soma to evoke a spike or burst response. Similar spikes arriving at different compartments would not be as effective in evoking a somatic response. Conversely, somatic spikes can back-propagate to the dendritic tree evoking dendritic spikes there.





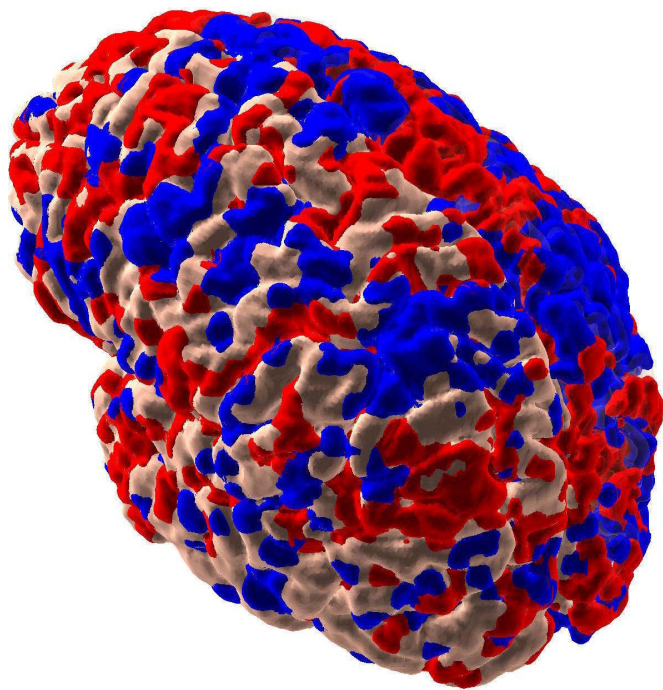


**Fig. 7.** Intrinsic correlations of fMRI signal between the seed cortical region in a location corresponding to posterior cingulate [data not shown; see Fox *et al.* (5)] and other regions in the model brain. Red (blue) voxels correspond to positive (negative) correlations ( $>1$  standard deviation of correlations of all voxels to the seed region). The right hemisphere is transparent so that inside voxels are visible.

measures are similar to propagating neocortical waves observed *in vitro* (28) and *in vivo* in visual cortex of anesthetized rats (29). They are slower than those *in vivo* in primary motor and dorsal premotor cortices of monkeys (30) and in turtle visual cortex (31).

**Functional Connectivity.** As suggested by studies of human subjects (5), we can analyze the resting state correlations of the simulated signals corresponding to fMRI (BOLD signals) on the slow time scales of minutes. Following Fox *et al.* (5), we collect signals (see *SI Appendix*) at each voxel of the cortical surface, low-pass filter them between 0.1 and 0.01 Hz, and then correlate the results with a seed region corresponding to posterior cingulate. Regions positively and negatively correlated with the seed region are depicted in red and blue, respectively, in Fig. 7. Our results resemble those seen in experimental brain studies of human (5) and theoretical studies (32), indicating that the resting state of the mammalian brain on this scale consists of multiple anticorrelated functional clusters.

## Discussion

One way to deepen our understanding of how synaptic and neuronal processes interact to produce the collective behavior of the brain is to develop large-scale, anatomically detailed models of the mammalian brain. We started with the thalamocortical system because it is necessary for human consciousness. Currently, we are at the stage of calibrating and further validating the model by determining to what extent its activity is similar to that recorded in the mammalian cortex after receipt of various input signals.

Even in the absence of external input, the distribution of firing rates among various types of neurons is similar to that recorded *in*

*vivo*: pyramidal neurons fire just a few spikes per second with the lowest firing rate observed in layer 2/3, whereas basket cells fire tens of spikes per second with the highest firing rate in layer 5 (33). Individual neurons exhibit somatic and dendritic spikes, forward- and back-propagation of spikes along the dendritic trees, and spike-timing-dependent plasticity that is coupled to the dendritic compartments rather than to the somatic spikes. The model spontaneously generated rhythms and propagating waves (Fig. 6) that had frequency distributions, spatial extents, and propagation velocities similar to those observed in mammalian *in vivo* recordings. In a fashion similar to human data, the simulated fMRI signal exhibited slow oscillations with multiple anticorrelated functional clusters (Fig. 7).

The computer model allowed us to perform experiments that are impossible (physically or ethically) to carry out with animals. For example, we put the model into the noiseless regime to demonstrate that it can produce self-sustained autonomous activity. We perturbed a single spike (34, 35) in this regime (out of millions) and showed that the network completely reorganized its firing activity within half a second. It is not clear, however, how to interpret this sensitivity in response to perturbations (Fig. 5). On one hand, one could say that this sensitivity indicates that only firing patterns in a statistical sense should be considered, and individual spikes are too volatile. On the other hand, one could say that this result demonstrates that every spike of every neuron counts in shaping the state of the brain, and hence the details of the behavior, at any particular moment. This conclusion would be consistent with the experimental observations that microstimulation of a single tactile afferent is detectable in human subjects (36), and that microstimulation of single neurons in somatosensory cortex of rats affects behavioral responses in detection tasks (37).

After development of a detailed, more complete brain model, one may simulate the effect of structural perturbations, such as lesions, strokes, and tumors, on the global dynamics, and compare the results with animal or human EEG/MEG data. By using DTI of patients with Alzheimer's disease, Parkinson's disease, or other neurological and psychiatric disorders, one may investigate how the connectivity alone modifies brain dynamics. Changing the neuronal parameters to simulate the effect of various pharmacological agents, one may study the effect of drugs (including addictive drugs) on the dynamics of the model to aid design of new therapeutic strategies against neurological disorders. By simulating the effect of cholinergic modulatory systems, one may induce sleep oscillations into the model and study the dynamics of the sleep state and its effect on synaptic plasticity, learning, and memory. Knowing the state of every neuron and every synapse in such a model, one may analyze the mechanisms involved in neural computations with a view toward development of novel computational paradigms based on how the brain works. Finally, by reproducing the global anatomy of the human thalamocortical system, one may eventually test various hypotheses on how discriminatory perception and consciousness arise.

**ACKNOWLEDGMENTS.** Data files of cortical microcircuitry were kindly provided by Tom Binzegger, Rodney J. Douglas, and Kevan A. C. Martin (Eth Zurich, Zurich, Switzerland). The simulations were performed by using two MRI DTI data files, one of the brain of the first author (E.M.I.) and the other provided by Gordon Kindlmann (Scientific Computing and Imaging Institute, University of Utah), and Andrew Alexander [W. M. Keck Laboratory for Functional Brain Imaging and Behavior, University of Wisconsin-Madison ([www.sci.utah.edu/gk/DTI-data/](http://www.sci.utah.edu/gk/DTI-data/))]. Jeff Krichmar, Botond Szatmary, Douglas Nitz, and Niraj Desai provided useful comments. The authors are especially grateful to Dr. Joe Gally, who suggested many important improvements to the manuscript. This work was supported by the Neurosciences Research Foundation and by National Science Foundation Grant CCF-0523156.

1. Lumer ED, Edelman GM, Tononi G (1997) Neural dynamics in a model of the thalamocortical system. I. Layers, loops and the emergence of fast synchronous rhythms. *Cereb Cortex* 7:207–227.

2. Lumer ED, Edelman GM, Tononi G (1997) Neural dynamics in a model of the thalamocortical system. II. The role of neural synchrony tested through perturbations of spike timing. *Cereb Cortex* 7:228–236.

